BRAIN
ORIGINAL ARTICLE

Double administration of self-complementary AAV9^{NDUFS4} prevents Leigh disease in *Ndufs4*$^{-/-}$ mice

Samantha Corrà,[1] Raffaele Cerutti,[1,2] Valeria Balmaceda,[1] Carlo Viscomi[3,4,†] and Massimo Zeviani[1,2,4,†]

[†]These authors contributed equally to this work.

Leigh disease, or subacute necrotizing encephalomyelopathy, a genetically heterogeneous condition consistently characterized by defective mitochondrial bioenergetics, is the most common oxidative-phosphorylation related disease in infancy. Both neurological signs and pathological lesions of Leigh disease are mimicked by the ablation of the mouse mitochondrial respiratory chain subunit Ndufs4$^{-/-}$, which is part of, and crucial for, normal Complex I activity and assembly, particularly in the brains of both children and mice. We previously conveyed the human *NDUFS4* gene to the mouse brain using either single-stranded adeno-associated viral 9 recombinant vectors or the PHP.B adeno-associated viral vector. Both these approaches significantly prolonged the lifespan of the *Ndufs4*$^{-/-}$ mouse model but the extension of the survival was limited to a few weeks by the former approach, whereas the latter was applicable to a limited number of mouse strains, but not to primates. Here, we exploited the recent development of new, self-complementary adeno-associated viral 9 vectors, in which the transcription rate of the recombinant gene is markedly increased compared with the single-stranded adeno-associated viral 9 and can be applied to all mammals, including humans. Either single intra-vascular or double intra-vascular and intra-cerebro-ventricular injections were performed at post-natal Day 1. The first strategy ubiquitously conveyed the human *NDUFS4* gene product in *Ndufs4*$^{-/-}$ mice, doubling the lifespan from 45 to ≈100 days after birth, when the mice developed rapidly progressive neurological failure. However, the double, contemporary intra-vascular and intra-cerebroventricular administration of self-complementary-adeno-associated viral NDUFS4 prolonged healthy lifespan up to 9 months of age. These mice were well and active at euthanization, at 6, 7, 8 and 9 months of age, to investigate the brain and other organs post-mortem. Robust expression of hNDUFS4 was detected in different cerebral areas preserving normal morphology and restoring Complex I activity and assembly. Our results warrant further investigation on the translatability of self-complementary-adeno-associated viral 9 NDUFS4-based therapy in the prodromal phase of the disease in mice and eventually humans.

1 Venetian Institute of Molecular Medicine, 35128 Padova, Italy
2 Department of Neurosciences, University of Padova, 35128 Padova, Italy
3 Department of Biomedical Sciences, University of Padova, 35131 Padova, Italy
4 Study Centre for Neurodegeneration, Univcersity of Padova (CESNE), 35131, Padova, Italy

Correspondence to: Massimo Zeviani, MD, PhD Professor
The Clinical School, University of Padova
Department of Neurosciences
Veneto Institute of Molecular Medicine
Padova 35128, Italy
E-mail: massimo.zeviani@unipd.it

Received February 04, 2022. Revised April 20, 2022. Accepted April 30, 2022

Correspondence may also be addressed to: Carlo Viscomi, PhD, Associate Professor
The Clinical School, University of Padova
Department of Biomedical Sciences
Padova 35131, Italy
E-mail: carlo.viscomi@unipd.it

Keywords: mitochondrial disease; *Ndufs4*; gene therapy; Complex I; Leigh disease

Abbreviations: AAV = adeno-associated virus; i.c.v. = intra-cerebro-ventricular; i.v. = intra-vascular; MRC = mitochondrial respiratory chain; P1 = post-natal Day 1

Introduction

Primary mitochondrial disorders are genetically defined as mutations in genes related to oxidative-phosphorylation (OXPHOS),[1] the pathway supplying most of the energy currency of the cell, i.e. ATP, in addition to production of heat and accomplishment of a number of additional, energy requiring, essential functions of the organelle.[2] Either mutations in the mitochondrial genome, or in OXPHOS-related nuclear genes can lead to mitochondrial disorders.[2] The clinical presentations are extremely variable, from single organ failure to multisystem disorders, as are the features characterizing adult-onset syndromes from infancy- or childhood-onset conditions. In paediatric cases, the outcome is frequently very severe, usually fatal, often dominated by multiple neurological failure, with the characteristic neuropathological and MRI features of Leigh disease.[3] Leigh disease is indeed a biochemically and genetically heterogeneous entity, being due to defects/mutations in single or combined mitochondrial respiratory chain (MRC) complexes. This includes defects in the activity of the corresponding MRC complexes, as well as a spectrum of defects of upstream mitochondrial bioenergetic pathways, such as the pyruvate dehydrogenase complex.[3] Despite a huge, long-standing effort in the last three decades, no effective therapy has been developed for most mitochondrial disorders, especially in children, with the exception of coenzyme Q treatment in specific defects of the biosynthesis of this important shuttle redox compound, which is part of the MRC, and idebenone, which shares structural and in part functional similarities to coenzyme Q.[4] Idebenone has been found moderately beneficial in Leber's Hereditary Optic Atrophy (LHON), a maternally inherited form of blindness due to degeneration of the retinal ganglia cells, caused by diverse mutations (three of which are predominant) in mtDNA genes.[5] The identification of an etiological cure for mitochondrial disorders is made even more difficult by the impossibility of any nucleic acid reaching the inner mitochondrial compartment where mtDNA resides, thus preventing the controlled manipulation of mtDNA mutations via homologous recombination.[6] The correction of mutant mtDNA by protein-based mitochondrial targeted 'editing devices' is actively experimented with by some centres worldwide.[7] In addition, a substantial fraction of mitochondrial disorders is still genetically undefined, since a relevant proportion of disease is due to mutations in OXPHOS-related nuclear genes,[8] replacement with wild-type versions of the culprit gene is a strategy that can nowadays take advantage from the development of numerous adeno-associated viral (AAV) serotypes able to target nucleus-encoded genes either ubiquitously or to specific organs. AAV vectors maintain the conveyed gene material as an episome construct that does not interfere, at least by any functional relevance, with the chromosomal genome.[9] Albeit safer than other approaches in which the recombinant gene is integrated in the nuclear genome of the host, the episomal distribution has an important limit, as it restrains the use of AAV recombinant vectors to post-mitotic or stable tissues. Another important limit is packaging constraint because big genes, such as *OPA1* or *POLG*, cannot be accommodated within the genomic structure of the vectors.[4] We have been using AAV8 vectors to convey to recombinant mouse model liver some genes whose absence determines the accumulation of toxic compounds for the organism, for instance the *ETHE1* gene, encoding a sulphide dioxygenase whose impairment is responsible for ethylmalonic encephalopathy,[10] or *TYMP*, encoding thymidine phosphorylase, the key enzyme for the clearance of thymidine and other pyrimidines that causes human mitochondrial neuro-gastro-intestinal encephalomyopathy.[11,12] We also used the same serotype to re-express *MPV17*, encoding a small hydrophobic protein of the inner mitochondrial membrane in the liver of *Mpv17*$^{-/-}$ mice, fully recovering the severe mtDNA depletion detected in hepatocytes of both humans and mice.[13] More recently, we developed AAV-based strategies to test gene replacement in *NDUFS4*$^{-/-}$ mice, a model of Leigh disease due to the lack of an accessory subunit of complex I[14] (in humans, its absence/impairment is in fact a rare cause of Leigh disease[15]). The *Ndufs4*$^{-/-}$ mice develop a post-weaning, early onset multiple neurological failure with severe ataxia, motor freezing and food avoidance, associated with profound decrease of Complex I activity, invariantly preceded by coat defluvium occurring once at ~15–20 days after birth. All mice die of neurological failure associated with massive brain spongiosis and necrosis, similar in part to the neuropathology of human Leigh disease, within 2 months after birth, with a median survival of 45 days. In a first set of experiments, we administered single-stranded (ss) recombinant AAV9 vectors expressing the human NDUFS4 protein by either intra-vascular (i.v.) injection only (10^{12} viral particles/individual), or i.v. and contemporary intra-cerebro-ventricular (i.c.v.) injection ($1.5–3 \times 10^{11}$ viral particles/individual) at post-natal Day 1 (P1).[16] While the i.v. treatment or the i.c.v. treatment alone gave mild improvement of the motor performance with no increase in the lifespan, the double, contemporary administration, i.v. and i.c.v. at P1 determined an increment of the lifespan by a few weeks accompanied by improved locomotor performance. Immunofluorescence-based experiments using a green fluorescent protein-expressing the ssAAV9 vector showed preferential localization of the viral particles and associated NDUFS4 protein in the astroglial cells of the brain, rather than in neurons, a phenomenon that can explain, at least in part, the limited efficacy of this treatment. In a second set of experiments, we i.v. treated at P28 our *Ndufs4*$^{-/-}$ animals with similarly recombinant PHP.B.[17] The age of administration was based on the observation that the phospho-inositol receptor (LY6H) that allows the PHP.B recombinant vector to cross the blood–brain barrier is expressed after weaning in mice. This treatment determined a substantial increase of the lifespan associated with diffuse distribution of the viral particles throughout the brain, including neurons. However, PHP.B

can be used only in a few strains of mice containing the phospho-inositol based receptor that is absent in other mouse strains, as well as primates.

We present here an important evolution of these first attempts, based on the use of self-complementary (sc), rather than ss, AAV9 vectors expressing the human NDUFS4 protein in different organs, including the brain.

Materials and methods

Animal work

All animal experiments were carried out in accordance with the EU Directive 2010/63/EU (authorization no. 474/2020-PR). The mice were kept on a C57BL/6 background, and wild-type (WT) littermates were used as controls. The animals were maintained in a temperature- and humidity-controlled animal care facility with a 12-h light/12-h dark cycle and free access to water and food, and they were monitored weekly to examine body condition, weight and general health. The mice were sacrificed by cervical dislocation at the time points indicated in the text for subsequent analysis.

Morphological analysis

For histological and immunohistochemical analyses, brains from scAAV9-hNDUFS4-treated and untreated animals were fixed for a few days in 10% neutral buffered formalin, and then processed on a Leica ASP300S tissue processor and infiltrated with Paraplast brand paraffin. All sections were cut on a Leica RM2245 microtome at a thickness of 4 μm. Haematoxylin and eosin staining was performed using a standard protocol. PathoGreen stain was performed by following the manufacturer's instructions. Immunohistochemistry was performed using a Novolink Polymer Detection System.

Vector construction and injection

hNDUFS4 was cloned into scAAV9-CAG vector. AAV titre was obtained by both dot blot and quantitative PCR. For i.v. injections, pups were injected with 40 μl AAV particles into the temporal vein, using a 31-gauge, 30° bevelled needle syringe. For i.c.v. injection, pups were injected with 4 μl AAV9 into one lateral ventricle, located 1 mm lateral to the superior sagittal sinus and 2 mm rostral to the transverse sinus, to a depth of 2 mm using an electrophysiology glass capillary connected to a sterile syringe.

Rotarod analysis

A rotarod apparatus (Ugo Basile) was used to assess coordination skills. After two acclimation sessions, the mice underwent three trial sessions at least 20 min apart, using a standard acceleration protocol.

Immunoblotting

Mouse tissues were homogenized in 10 volumes of 10 mM potassium phosphate buffer (pH 7.4). Mitochondrial-enriched fractions were collected after centrifugation at 800*g* for 10 min in the presence of protease inhibitors, and frozen and thawed three times in liquid nitrogen. Protein concentration was determined by the Lowry method. Aliquots of 30 μg each were run through a 4–12% sodium dodecyl sulphate-polyacrylamide gel electrophoresis and electroblotted onto a polyvinylidene fluoride membrane, which was then immunodecorated with different antibodies.

Blue-native gel electrophoresis

Isolated mitochondria were resuspended in 1.5 M aminocaproic acid, 50 mM Bis–Tris/HCl pH 7.0. The samples were solubilized with 4 mg of *n*-dodecyl β-D-maltoside (Sigma) per mg of protein. After 5 min of incubation on ice, samples were centrifuged at 18 000*g* at 4°C for 10 min. The supernatant was collected and resuspended with Sample Buffer (750 mM aminocaproic acid, 50 mM Bis–Tris/HCl pH 7.0, 0.5 mM EDTA and 5% Serva Blue G). Native samples were separated by 3–12% gradient blue-native gel electrophoresis and then electroblotted on polyvinylidene fluoride membrane membranes for immunodetection.

Genome DNA extraction and quantitative PCR

Total DNA was extracted from frozen tissues. SYBR-GREEN-based real-time quantitative PCR Invitrogen (Promega) was carried out for AAV-copy number analysis as previously described,[17] using primers specific to both human and murine *NDUFS4* genes; the *RNAseP* gene was used as a reference.

Biochemical analysis

Tissues were snap-frozen in liquid nitrogen and homogenized in 10 mM phosphate buffer (pH 7.4). The spectrophotometric activity of cI, as well as citrate synthase, was measured as previously described.[17]

Reagents

Antibodies used included: anti-NDUFS4 (1:100 for immunohistochemistry and 1:1000 for western blot) was from Novus Biologicals (catalogue no. NBP1-31465); anti-CD68 (1:250) was from ABCAM; anti-GFAP (1:1000) was from Sigma; anti-NDUFA9, and anti- succinate dehydrogenase B (1:1000) were from MitoSciences (catalogue no. ab14713). Secondary antibodies were from Promega [catalogue nos. W4011 (rabbit) and W4021 (mouse)].

Statistical analysis

All numerical data are expressed as mean ± SEM. Student's unpaired two-tail *t*-test and Kaplan–Meier distribution were used for statistical analysis. Differences were considered statistically significant for $P < 0.05$.

Data availability

The authors confirm that the data supporting the findings of this study are available within the article and the Supplementary material.

Raw data were generated at Veneto Institute of Molecular Medicine and are available from the corresponding authors on request.

Results

Single treatment

The scAAV9 vector contains a double-stranded (self-complementary, sc) genome compared to the single-stranded genome of the original ssAAV vectors, which confers to this variant a substantial increase in the transcription efficiency of the inserted gene of interest. The scAAV9 vector has been used to set up a successful gene replacement therapy of the *SMN1* cDNA, a gene

missing in and causing the spinal muscular atrophy spectrum, via i.v. and intra-rachideal injection, and even more recently only through intra-rachideal administration. However, it has never been tested in mitochondrial disease models.

We first treated four *Ndufs4*$^{-/-}$ P1 pups with 10^{11} scAAV9 viral units containing the human *NDUFS4* cDNA. This dosage was chosen since a previous attempt on two P1 *Ndufs4*$^{-/-}$ pups i.v. treated with 3.5×10^{10} virions was scarcely effective *in vivo* (Supplementary Fig. 1). The hNDUFS4 protein is almost identical to the mouse (m) NDUFS4 protein (88% identity; 94% similarity), displaying 22 changes, 14 of which occur in the predicted mitochondrial targeting sequence at the N terminus. In numerous previous experiments performed by us and elsewhere, the hNDUFS4 protein appears to be incorporated and be able to restore the missing original murine Ndufs4 subunit in *Ndufs*$^{4-/-}$ cells and individuals.[16]

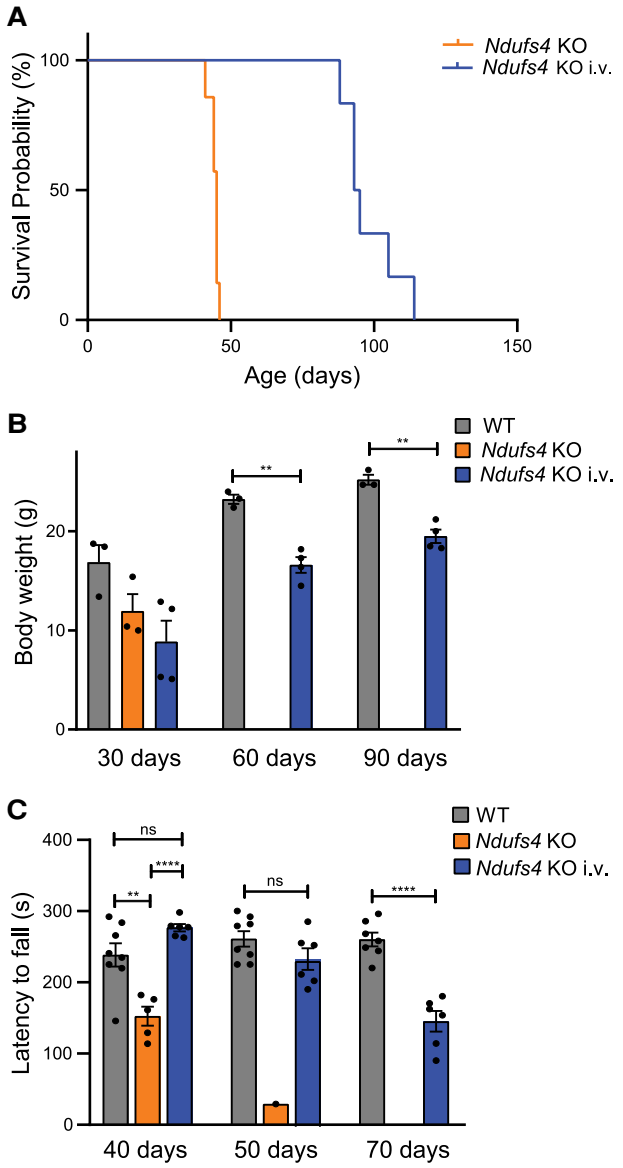

Figure 1 Clinical characterization of scAAV9^{NDUFS4} i.v.-treated newborn mice. (**A**) Kaplan–Meier survival probability in *Ndufs4*$^{-/-}$ (orange; $n = 7$), scAAV9 i.v.-treated *Ndufs4*$^{-/-}$ (blue; $n = 6$). Significance was calculated with a log rank test (median lifespan 45 for *Ndufs4*$^{-/-}$ versus 94 days for scAAV9^{NDUFS4}; $P < 0.001$). (**B**) Variation in body weights over time in WT (grey; $n = 6$), *Ndufs4*$^{-/-}$ (orange; $n = 6$), scAAV9^{NDUFS4} i.v.-treated *Ndufs4*$^{-/-}$ (blue; $n = 6$). Error bars represent ± SEM. (**C**) Rotarod performance in WT (grey; $n = 8$), *Ndufs4*$^{-/-}$ (orange; $n = 6$), scAAV9 i.v.-treated *Ndufs4*$^{-/-}$ (blue; $n = 6$) mice. At 70 days no *Ndufs4*$^{-/-}$ mice were alive. The bars represent mean ± SEM. $^{*}P < 0.05$, $^{**}P < 0.01$, $^{***}P < 0.001$ and $^{****}P < 0.0001$ calculated by unpaired, Student's two-tailed *t*-test.

The i.v. treatment with 10^{11} scAAV9 recombinant viral units prevented the coat *defluvium* (Fig. 1A) and prolonged the lifespan significantly, up to 90–110 days. This is displayed in the Kaplan–Meier graph in Fig. 1B (log rank $P = 0.001$). Nevertheless, all the treated animals, which appeared healthy and well during most of their lifetime, with a gain of body weight similar to controls (Fig. 1C), manifested, in the last 2 days before euthanasia, the onset of ataxic gait, followed by locomotor freezing and food avoidance with loss of >15% body weight (the limit for humane culling according to our ethical licence). The motor coordination of AAV-treated mice, measured by rotarod tests, showed a decline in the motor skills, comparable to controls at 40 days, moderately reduced at 50 days and significantly reduced at 70 days (Fig. 1D). Untreated *Ndufs4*$^{-/-}$ had a 50% reduction in the rotarod performance at post-natal Day 40, and the only one individual living up to 50 days could barely stay on the rotating bar (Fig. 1D). The number of viral units per cell was measured post-mortem by quantitative PCR of the viral genome, being ~1–2 copies/cell in brain and heart and 3–4 copies/nucleus in skeletal muscle (Fig. 2A). Notably, three WT animals injected with the same amount of virus did not show any toxicity for up to 6 months. The human NDUFS4 protein expressed in treated wild-type and knockout animals was clearly detectable in brain homogenates by western blot immune-visualization, similar to the murine endogenous protein detected in control littermates (Fig. 2B). Likewise, immunoreactivity specific to NDUFS4 was detected in various brain areas of treated animals and was comparable with that shown in corresponding brain areas of controls (Supplementary Fig. 2). However, neuropathology analysis of the terminally ill, treated individuals revealed the presence of areas of neuronal loss and neurodegeneration, spongiotic changes in the neuropilum, moderate reactive astrogliosis and scattered microglial foci. These lesions were in fact more severe than those observed in untreated animals, possibly because the latter had a much shorter lifespan and could not develop full-blown lesions which instead became manifested in the treated, longer surviving ones. The most affected areas of the AAV9-treated brains included the olfactory bulb, thalamus and striatum. The areas of neurodegeneration were intensely fluorescent by PathoGreen staining (Fig. 3 and Supplementary Fig. 3).

Biochemically, brain homogenates from AAV9-treated *Ndufs4*$^{-/-}$ mice had Complex I/Citrate synthase activity comparable to that of untreated WT mice (Fig. 4A), whereas it was virtually absent in naïve *Ndufs4*$^{-/-}$ mice. In the AAV9-treated *Ndufs4*$^{-/-}$ mice we observed a robust staining of the band corresponding to native Complex I by in-gel activity, compared with the controls (Fig. 4B). However, western blot immune-visualization of blue-native gel electrophoresis showed the persistence of a well-known 830 kDa band (Fig. 4C), in addition to fully assembled >1 MDa band, which was previously proven to correspond to the Complex I lacking the N module.[18] This band was the only Complex I-cross reacting material visualized in the lanes of naïve untreated *Ndufs4*$^{-/-}$ littermates, which completely lack fully assembled Complex I (Fig. 4B).

Double treatment

Albeit encouraging, the results obtained by i.v. treatment led to moderate survival, by just 3–4 months beyond the survival median

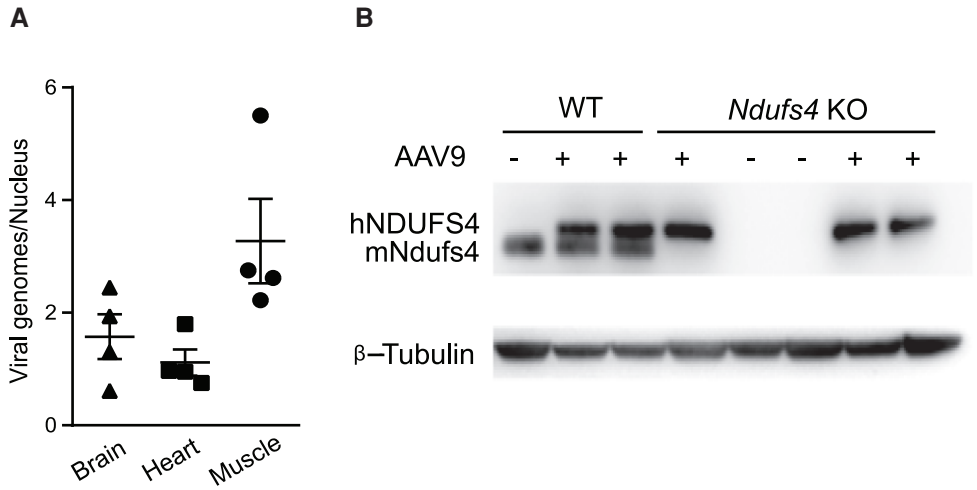

Figure 2 Molecular characterization of scAAV9^{NDUFS4} i.v.-treated newborn mice. (**A**) Viral genome copies content in tissues from AAV9-treated *Ndufs4*$^{-/-}$ mice ($n = 4$). Error bars indicate the ±SEM. (**B**) Western blot analysis of brain homogenates. β-tubulin was used as protein-loading standard.

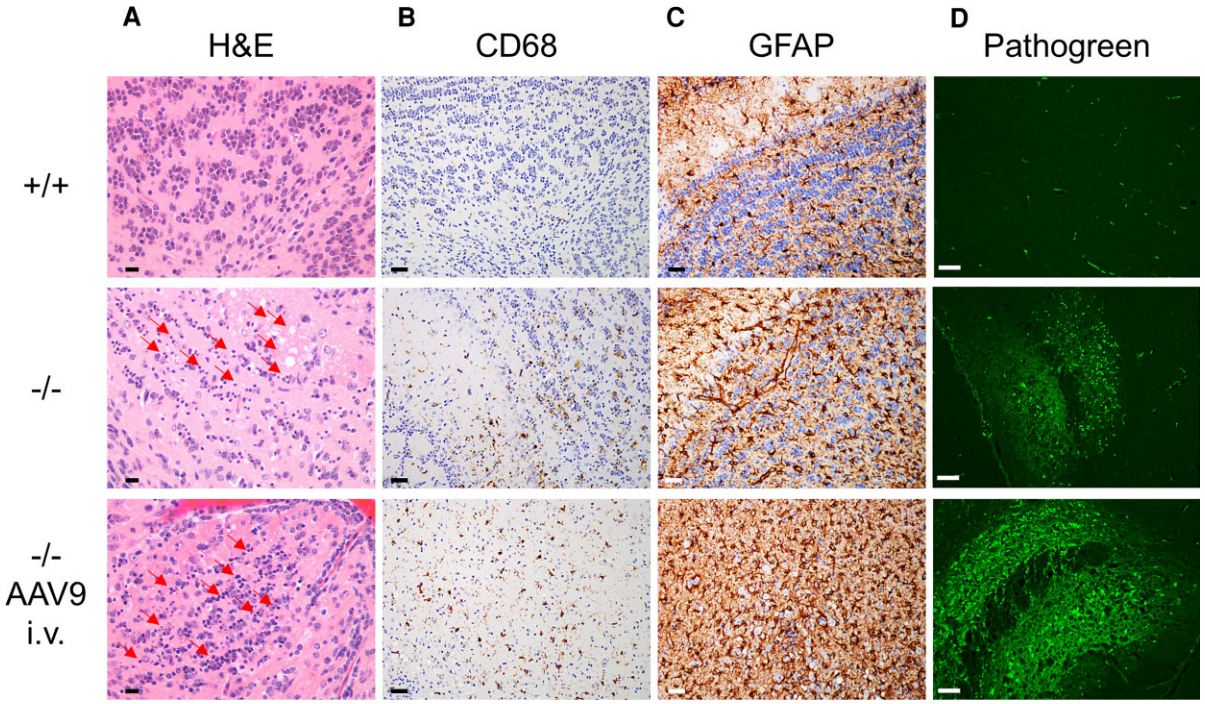

Figure 3. Profound alterations in the olfactory bulb from mice injected with a single dose of scAAV9-*hNDUFS4*. (**A**) Haematoxylin and eosin staining. Note the presence of degenerated neurons and spongiotic changes (red arrows) in the olfactory bulb of both untreated and treated $^{-/-}$ animals compared with the $^{+/+}$ control. Scale bars, 10 µm. (**B**) Analysis of microgliosis by immunohistochemical staining with an anti-CD68 antibody reveals the presence of numerous dark brown activated microglial cells. Scale bars, 40 µm. (**C**) Analysis of astrogliosis using an antibody against the GFAP protein. Scale bars, 40 µm. (**D**) PathoGreen staining. Note the presence of a lot of degenerated cells in the olfactory bulb of the injected animal. Scale bars, 50 µm.

of naïve untreated littermates. The reasons for the limited effects of the i.v. treatment are unclear, since we demonstrated that the recombinant protein was in fact present in the brain, and assembled Complex I was detected, despite the coexistence of an aliquot of partially assembled Complex I, missing the N module. It is of course possible that this rather coarse inspection missed the effective, detailed distribution of the therapeutic gene, which may have still been uneven, as demonstrated previously by using ssAAV9^{NDUFS4} vectors.[16] This would explain the presence of patchy, severe lesions, concentrated in specific areas of the brain of the euthanized i.v. treated animals (e.g. the olfactory bulb, Fig. 3). We tried to circumvent the limited improvement of the clinical outcome in our *Ndufs4*$^{-/-}$ animals by increasing brain targeting of the recombinant vector through a double administration protocol in five P1 *Ndufs4*$^{-/-}$ animals, i.e. 10^{11} i.v. injected viral particles and 10^{10} viral particles introduced via intra-cerebral-ventricle (i.c.v.) injection through intra-thecal puncture. One animal died at 85 days of life with neurological symptoms and neuropathology similar to those of animals receiving the i.v. treatment only (Supplementary Fig. 4). The other four mice remained in healthy conditions as confirmed by

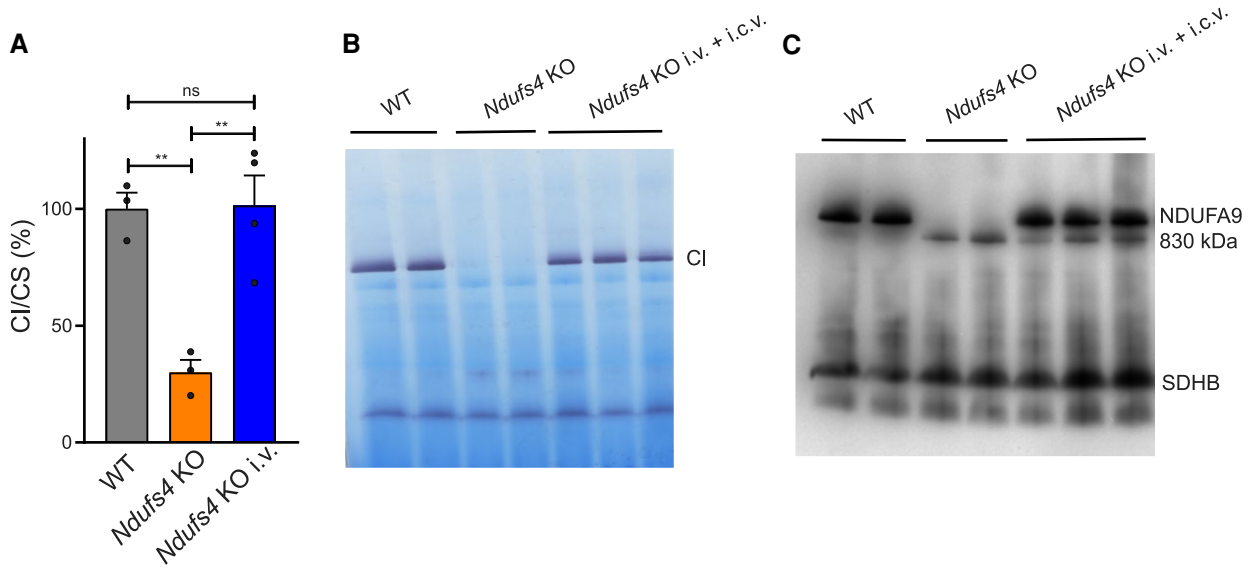

Figure 4 Biochemical characterization of scAAV9^{NDUFS4} i.v.-treated newborn mice. (**A**) Spectrophotometric activity of Complex I (CI) in brain homogenates from WT mice (grey; $n = 3$), *Ndufs4*$^{-/-}$ (orange; $n = 3$) and AAV-treated *Ndufs4*$^{-/-}$ mice (blue; $n = 4$) expressed as percentage of CI/citrate synthase (CS). Bars indicate ±SEM. The asterisks represent the significance levels calculated by unpaired, Student's two-tailed *t*-test: $^{*}P < 0.05$, $^{**}P < 0.01$ and $^{***}P < 0.001$. (**B**) In-gel activity for Complex I. Note the complete absence of the Complex I band in *Ndufs4*$^{-/-}$ samples. (**C**) Western blot (WB) analysis of first-dimension blue-native gel electrophoresis on brain mitochondria with an antibody specific for Complex I (NDUFA9). Note that only the 830-kDa subassembly band is present in *Ndufs4*$^{-/-}$ samples, while both fully assembled and subassembly bands are present after treatment with scAAV9^{NDUFS4}. An antibody specific for Complex II was used as control (succinate dehydrogenase B).

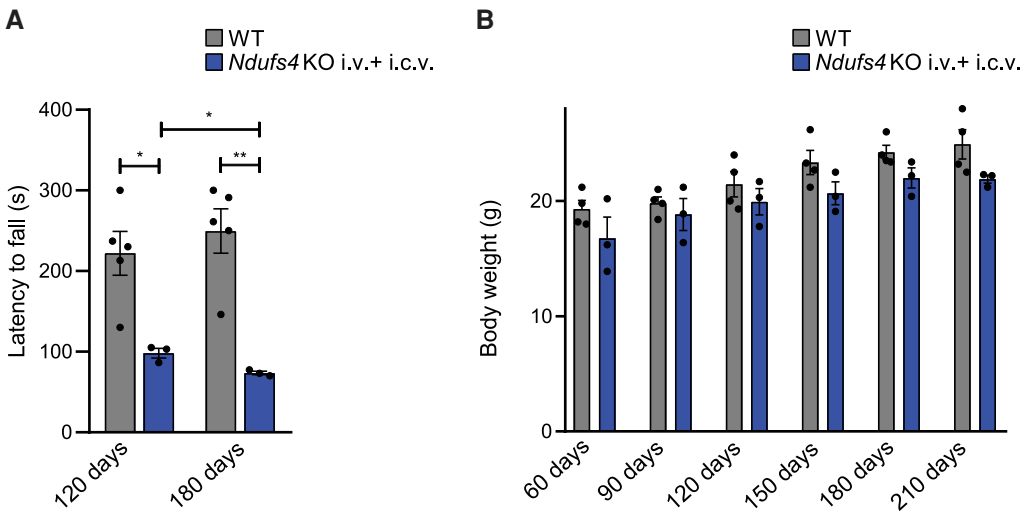

Figure 5 Clinical characterization of scAAV9^{NDUFS4} i.v./i.c.v.-treated newborn mice. (**A**) Rotarod analysis in WT (grey; $n = 5$) and scAAV9^{NDUFS4} i.v./i.c.v.-treated *Ndufs4*$^{-/-}$ (blue; $n = 4$) mice. Error bars represent ±SEM. The asterisks indicate the significance levels calculated by unpaired, Student's two-tailed *t-test*: $^{*}P < 0.05$ and $^{**}P < 0.01$. One animal was an outlier according to Grubbs test and was excluded from the analysis. (**B**) Variation of body weights over time in WT (grey; $n = 4$), scAAV9^{NDUFS4} i.v.+i.c.v.-treated *Ndufs4*$^{-/-}$ (blue; $n = 3$) mice. Error bars represent ±SEM. The asterisks represent the significance levels calculated by unpaired, Student's two-tailed *t*-test: $^{*}P < 0.05$, $^{**}P < 0.01$ and $^{***}P < 0.001$.

daily inspection, bi-weekly body weight measurement and quantitative locomotor *in vivo* analysis. Weekly performed rotarod tests showed that one mouse was able to walk on the rotating rod for >200 s, whereas the other three mice endured on the rotating rod for 85–105 s. A Grubbs test revealed that the highly performing mouse was an outlier and was therefore excluded from the analysis (Fig. 5A). We detected a slight but significant decline of the performance over time at 120 and 180 days of age, when all the animals were still alive. Likewise, there was no significant difference in the body weight among the four long-surviving animals in comparison with the littermate controls (Fig. 5B). In contrast, the double injected individual euthanized at 85 days was always smaller than the littermates (his body weight was 10 g at 80 days of age) and declined suddenly to very poor conditions, prompting us to euthanasia. Histological analysis of heart and kidney did not show any alteration, whereas the liver showed extensive apoptosis, which was further confirmed by immune-decoration with anti-cleaved caspase 3 antibody (Supplementary Fig. 5). The four healthy, doubly treated *Ndufs4*$^{-/-}$ animals were eventually euthanized at 6, 7, 8 and 9 months after birth, respectively. Fig. 6A shows

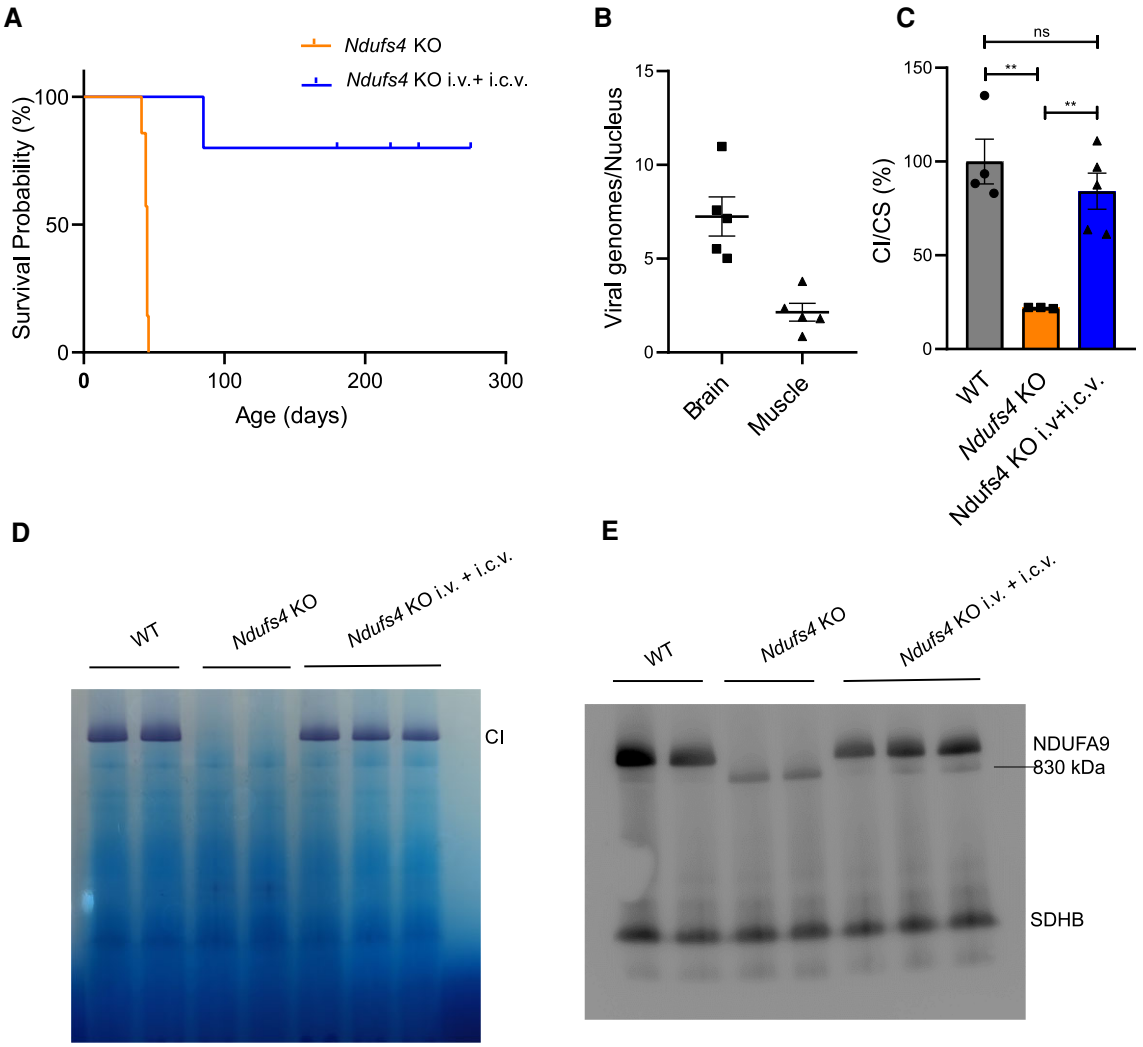

Figure 6 Molecular characterization of scAAV9^{NDUFS4} i.v./i.c.v.-treated newborn mice. (**A**) Kaplan–Meier survival probability in *Ndufs4*$^{-/-}$ (orange; $n = 6$), scAAV9^{NDUFS4} i.v./i.c.v.-treated *Ndufs4*$^{-/-}$ (blue; $n = 5$). Log rank test = 0.001. (**B**) Viral genome copies content in brain from AAV-treated *Ndufs4*$^{-/-}$ mice ($n = 5$). Error bars indicate the ±SEM. (**C**) Spectrophotometric activity of Complex I (CI) in brain homogenates from *Ndufs4*$^{+/+}$ mice (grey; $n = 3$), *Ndufs4*$^{-/-}$ (orange; $n = 3$) and AAV-treated *Ndufs4*$^{-/-}$ mice (blue; $n = 4$) expressed as percentage of CI/citrate synthase (CS). Bars indicate ± SEM. $^{*}P < 0.05$, $^{**}P < 0.01$ and $^{***}P < 0.001$ calculated by unpaired, Student's two-tailed *t*-test. (**D**) In-gel activity for CI. Note the complete absence of the CI band in *Ndufs4*$^{-/-}$ samples. (**E**) Western blot (WB) analysis of first-dimension blue-native gel electrophoresis on brain mitochondria with an antibody specific for CI (NDUFA9). Note that only the 830-kDa subassembly band is present in *Ndufs4*$^{-/-}$ samples, while both fully assembled and subassembly bands are present after treatment with scAAV9^{NDUFS4}. An antibody specific for Complex II was used as control (succinate dehydrogenase B).

the Kaplan–Meier survival probability graph, which gave a log rank test of 0.001 in comparison to the survival probability of untreated naïve *Ndufs4*$^{-/-}$ littermates. Therefore, this protocol allowed the survival in good-health conditions of the *Ndufs4*$^{-/-}$ mice to ages well beyond those of both naïve untreated and i.v. treated animals. We euthanized our doubly treated animals to analyse over time the biochemical, morphological and genetic features compared to controls. Following the 3R rule, we limited the number of treated animals to five, since in no case naïve, untreated *Ndufs4*$^{-/-}$ mice have ever survived beyond 65 days after birth in our cohort or elsewhere, and no long-surviving outlier has ever been reported in the literature with values even distantly similar to those presented here. Not surprisingly, the difference between doubly treated versus untreated animals was statistically highly significant (Fig. 6A).

Biochemical evaluation included the measurement of the viral copy number, which was ∼7 copies/cell in the brain, specifically in the forebrain, therefore much more than in animals receiving the i.v. only treatment (Fig. 6B). In skeletal muscle, the viral copy number was ∼3–4 copies/nucleus, i.e. similar to the results obtained in the i.v. only treated animals. However, seven copies/cell were also present in the individual that became sick and died at 85 days, suggesting that the viral copy number is not the only parameter that can determine the observed, substantial prolongation of health and lifespan in the doubly treated animals. The Complex I/citrate synthase activity was not significantly different from and in fact comparable to that of age-matched controls (Fig. 6C). Blue-native gel electrophoresis WB immune-visualization showed the presence of fully assembled, in-gel-active, Complex I, with the notable virtual absence of the 830 kDa band that was prominent in the naïve untreated animals in which assembled Complex I was undetectable (Fig. 6D and E), as well as in i.v. only treated individuals. Importantly, the morphological analysis of the brain in the four healthy animals was normal, and comparable to that of age-matched controls (Fig. 7), in contrast with the several

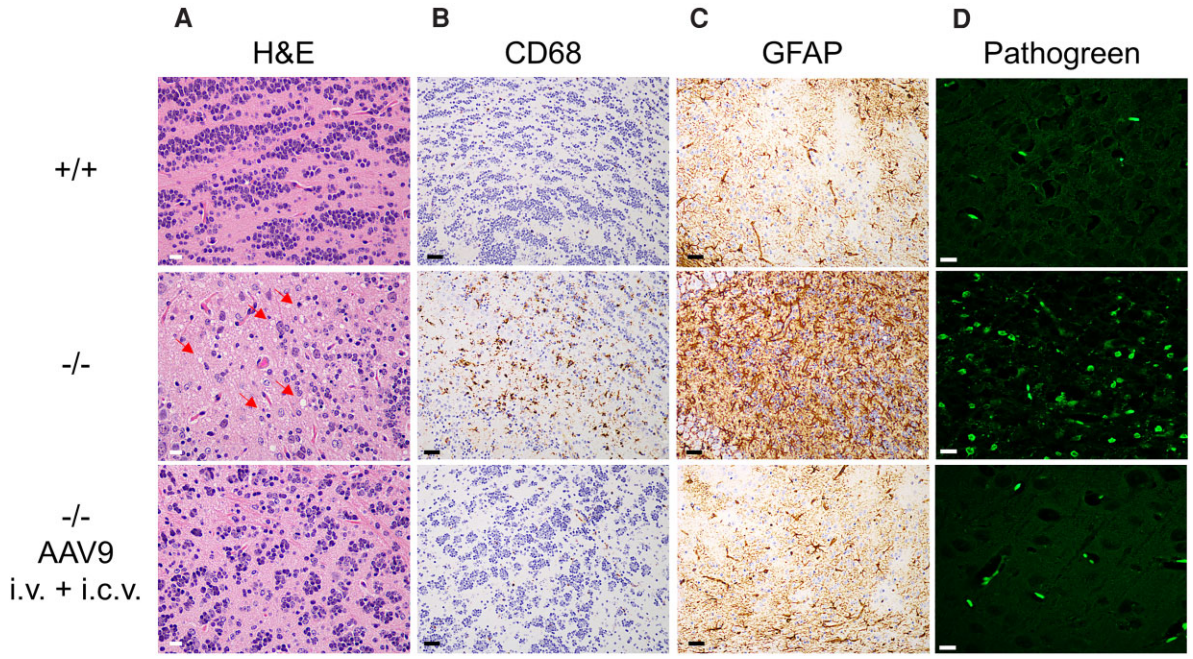

Figure 7. Restoration of NDUFS4 expression in the brain. scAAV9^{NDUFS4} prevented microgliosis, atrogliosis and neuronal degeneration in the olfactory bulb from mice subjected to a double i.v. +/+ i.c.v. administration of scAAV9^{NDUFS4}. (**A**) Haematoxylin and eosin staining. Note the presence of spongiosis and degenerated neurons (red arrows) in the olfactory bulb of the untreated animal that are absent in scAAV9^{NDUFS4}-treated animals. Scale bars, 10 µm. (**B**) Immunohistochemistry using an antibody against CD68 shows the presence of brown activated microglial cells in the olfactory bulb of the untreated animals that are absent in the treated animal. Scale bars, 10 µm. (**C**) Analysis of astrogliosis by immune-decoration with an anti-GFAP antibody. Scale bars, 10 µm. (**D**) PathoGreen staining showing the absence of degenerated neurons in the scAAV9^{NDUFS4}-treated animal. Scale bars, 10 µm.

lesions found in the one individual deceased at 85 days, whose neuropathology was similar to that of i.v. only treated animals. Other organs, including heart, liver and kidney, did not show any gross abnormalities by haematoxylin and eosin staining (Supplementary Fig. 6).

Discussion

Mitochondrial disorders are devastating conditions, particularly in infants and children, for which no effective cure is currently available. Subacute necrotizing encephalomyelopathy, or Leigh disease, is the most common neuropathological, neuroimaging and clinical mitochondrial disease in infancy, characterized by a free post-natal window followed by the arrest and regression of neurodevelopmental milestones, with multiple failure of the functions associated with the brainstem nuclei, long ascending and descending tracts from and to the spinal cord, and other clinical signs caused by impaired truncal-bulbar and cerebellar functions (e.g. apnoeic episodes, abnormalities of coordination, posture and gait, persistent vomiting, seizures or myoclonic episodes, sometimes oculomotor impairment and optic atrophy with poor vision or blindness, etc.).[3] These clinically complex, evolutive features, which ultimately lead the affected children to die for global neurological failure, are associated with the early onset of necrotic, symmetrical lesions in the grey nuclei and surrounding white matter of brainstem, cerebellum, diencephalon, striatum and eventually the cortical ribbon, with gliosis, capillary proliferation and, often, patchy microglial infiltrates and spongiotic degeneration of the neuropilum.[18] The genetic basis of Leigh disease is highly heterogeneous, but converging on impairment of cell bioenergetics, mainly provided by mitochondrial metabolism. Thus, Leigh disease can be found in early onset, severe isolated defects of MRC Complex I, Complex IV, combined MRC defects, impaired proton flow through the channel associated with the ATP synthase, i.e. the A protein subunit encoded by MT-*ATPase6*, abnormalities of pyruvate dehydrogenase, particularly of the X-linked gene encoding the alpha subunit, and others.[18] These clinical and neuropathological lesions are mimicked by the *Ndufs4*$^{-/-}$ mouse, created several years ago and used in a number of experiments,[14,19] which lacks a small, accessory but neurologically essential subunit of Complex I, whose activity and assembly are severely reduced in the brain of these animals, as well as in the rare patients with loss of the same gene.[18] We used scAAV9 vector to ubiquitously convey the human NDUFS4 gene product, a protein highly similar to the murine ortholog, in *Ndufs4*$^{-/-}$ mice. The use of human genes in preclinical experiments is not uncommon[20] because this approach facilitates the translation of the very same vector to the patients. The i.v. administration at P1 let viral particles to cross the blood–brain barrier, express the recombinant NDUFS4 protein in nerve cell cytoplasm, as well as in other organs of the mouse, and prolong the health and wellbeing of the animals until ~100 days after birth, a lifespan twice as long as the lifespan of the naïve untreated *Ndufs4*$^{-/-}$ littermates whose median survival is 45 days. However, the clinical conditions of these animals had a fulminant deterioration within the final couple of days, leading them to be humanely euthanized when the loss of body weight overcame 15%. The mechanistic reasons for such an outcome are unclear, because immunodetection by western blot and immunohistochemistry did reveal the presence of the recombinant protein in different brain areas of the treated animals. Nevertheless, the viral copy number was relatively low (1 copy/cell on average), despite high dosage of the treatment (>10^{12} viral particles). It is possible that the protein remains, at this dosage, still unevenly distributed and therefore fails to compensate the

bioenergetic requests of crucial areas, e.g. the prominent olfactory bulb of the mouse, the vestibular nuclei, the striatum, which overtime can undergo neurodegeneration with neuronal loss, microvacuolization and pathosis of nerve cells, spongiotic alterations of the neuropilum, and microglial infiltration, as observed post-mortem in these animals.

Based on previous results obtained with ss AAV9^{NDUFS4} recombinant vectors[16] we then adopted a protocol including contemporary, double administration of recombinant scAAV9^{NDUFS4}, by both i.v. and i.c.v. injections at P1. Although one mouse died at 85 days, similar to the i.v.-only treated individuals, the remaining four doubly treated animals lived for several months in healthy, active conditions, with weight gain similar to controls and relatively preserved locomotor skills and coordination. They were in fact well and active when they were sacrificed at 6, 7, 8 and 9 months of age to investigate their biochemistry, genetics and morphology in brain and extraneurological organs. This analysis demonstrated robust expression of *NDUFS4* in different cerebral areas, preservation of normal morphology and maintenance of normal activity and assembly of Complex I. The extraneurological organs, including skeletal muscle, heart, liver and kidneys showed preserved morphology and the presence of fully assembled Complex I with normal activity, therefore suggesting a ubiquitous distribution and effect of the scAAV9^{NDUFS4} via i.v. injection. Our results clearly indicate that the concomitant boost of additional scAAV9^{NDUFS4} in the brain via the i.c.v. route can supply the brain of affected animals with a much higher virion copy number than the sole i.v. injection (7 versus 1) and that this quantitative difference warrants the long-standing permanence of the curative gene, and its expression, in all or most of the brain areas of the treated individuals. Nevertheless, we had one doubly treated mouse that succumbed at 85 days in poor clinical conditions, with neuropathological findings similar to the i.v.-only treated animals. This result stands as an important warning on the possibility that, for errors in the i.v. or i.c.v. administration of the vector, *in utero* developmental defects reducing the efficacy of the compensation operated by the gene replacement procedure, or specific (and still unknown) genetic background variants that may interfere with the functional complementation of the therapy, some individuals can display a refractoriness to the curative action of our gene therapy approach, with outcomes that are not entirely meeting the desired goal, i.e. the radical and prolonged cure *in vivo* of the clinical consequences caused by a crippled OXPHOS-related gene. Nevertheless, the spectacular results obtained in four out of five doubly treated animals prompt us to further investigate the potential translatability of scAAV9-based therapy, for instance by deferring the treatment to the prodromal phase of the disease in mice, to be in closer proximity with the real situations occurring with Leigh disease in children. Ultimately, we want to further explore the possibility to adopt the proposed protocol not only for replacing the *Ndufs4* gene but also other nucleus-encoded genes known to be responsible of Leigh disease, as recently shown for a *Surf1*$^{-/-}$ model generated by us and treated elsewhere with a single intra-thecal injection at 4 weeks after birth of a scAAV9^{SURF1} vector.[21] Alternatively, the direct administration of *Ndufs4* RNA can be considered, given the important results recently obtained by an approach, termed selective endogenous encapsidation for cellular delivery. Selective endogenous encapsidation for cellular delivery exploits the capacity of some retroviral-like proteins to secrete its own mRNA, opening the possibility to exploit them to deliver functional mRNA cargos to mammalian cells.[22]

If these preclinical experiments on animal models will be successful, the obvious step to follow would be the translation of these procedures to patients.

Acknowledgements

We thank Dr Michele Brischigliaro, PhD for technical support.

Funding

Our work is supported by: Telethon Foundation (GGP19007 to M.Z. and GGP20013 to C.V.); Fondation NRJ pour les Neurosciences - Institute de France Grant (to M.Z.); Associazione Luigi Comini Onlus (to M.Z. and C.V.), Association Française contre les Myopathies (23706 to C.V.).

Competing interests

The authors report no competing interests.

Supplementary material

Supplementary material is available at *Brain* online.

References

1. Gorman GS, Chinnery PF, DiMauro S, *et al*. Mitochondrial diseases. *Nat Rev Dis Primers*. 2016;2:16080.
2. Wallace DC. Mitochondrial genetic medicine. *Nat Genet*. 2018;50:1642–1649.
3. Walker MA, Miranda M, Allred A, Mootha VK. On the dynamic and even reversible nature of Leigh syndrome: Lessons from human imaging and mouse models. *Curr Opin Neurobiol*. 2021;72:80–90.
4. Viscomi C, Zeviani M. Strategies for fighting mitochondrial diseases. *J Intern Med*. 2020;287:665–684.
5. Zeviani M, Carelli V. Mitochondrial retinopathies. *Int J Mol Sci*. 2021;23:210.
6. Gammage PA, Moraes CT, Minczuk M. Mitochondrial genome engineering: The revolution may not be CRISPR-Ized. *Trends Genet*. 2018;34:101–110.
7. Silva-Pinheiro P, Minczuk M. The potential of mitochondrial genome engineering. *Nat Rev Genet*. 2021;23:199–214.
8. Gusic M, Prokisch H. Genetic basis of mitochondrial diseases. *FEBS Lett*. 2021;595:1132–1158.
9. Riyad JM, Weber T. Intracellular trafficking of adeno-associated virus (AAV) vectors: challenges and future directions. *Gene Ther*. 2021;28:683–696.
10. Di Meo I, Auricchio A, Lamperti C, Burlina A, Viscomi C, Zeviani M. Effective AAV-mediated gene therapy in a mouse model of ethylmalonic encephalopathy. *EMBO Mol Med*. 2012;4:1008–1014.
11. Torres-Torronteras J, Cabrera-Pérez R, Vila-Julià F, *et al*. Long-term sustained effect of liver-targeted adeno-associated virus gene therapy for mitochondrial neurogastrointestinal encephalomyopathy. *Hum Gene Ther*. 2018;29:708–718.
12. Torres-Torronteras J, Viscomi C, Cabrera-Pérez R, *et al*. Gene therapy using a liver-targeted AAV vector restores nucleoside and nucleotide homeostasis in a murine model of MNGIE. *Mol Ther*. 2014;22:901–907.
13. Bottani E, Giordano C, Civiletto G, *et al*. AAV-mediated liver-specific MPV17 expression restores mtDNA levels and prevents diet-induced liver failure. *Mol Ther*. 2014;22:10–17.
14. Kruse SE, Watt WC, Marcinek DJ, Kapur RP, Schenkman KA, Palmiter RD. Mice with mitochondrial complex I deficiency develop a fatal encephalomyopathy. *Cell Metab*. 2008;7:312–320.
15. Petruzzella V, Vergari R, Puzziferri I, *et al*. A nonsense mutation in the NDUFS4 gene encoding the 18 kDa (AQDQ) subunit of complex I

abolishes assembly and activity of the complex in a patient with Leigh-like syndrome. *Hum Mol Genet*. 2001;10:529–535.
16. Di Meo I, Marchet S, Lamperti C, Zeviani M, Viscomi C. AAV9-based gene therapy partially ameliorates the clinical phenotype of a mouse model of Leigh syndrome. *Gene Ther*. 2017;24:661–667.
17. Silva-Pinheiro P, Cerutti R, Luna-Sanchez M, Zeviani M, Viscomi C. A single intravenous injection of AAV-PHP.B-hNDUFS4 ameliorates the phenotype of Ndufs4-/- mice. *Mol Ther Methods Clin Dev*. 2020;17:1071–1078.
18. Ogilvie I, Kennaway NG, Shoubridge EA. A molecular chaperone for mitochondrial complex I assembly is mutated in a progressive encephalopathy. *J Clin Invest*. 2005;115:2784–2792.
19. van de Wal M, Adjobo-Hermans M, Keijer J, *et al*. Ndufs4 knockout mouse models of Leigh syndrome: Pathophysiology and intervention. *Brain*.2021;29:awab426.
20. Foust KD, Wang X, McGovern VL, *et al*. Rescue of the spinal muscular atrophy phenotype in a mouse model by early postnatal delivery of SMN. *Nat Biotechnol*. 2010;28:271–274.
21. Ling Q, Rioux M, Hu Y, Lee M, Gray SJ. Adeno-associated viral vector serotype 9-based gene replacement therapy for SURF1-related Leigh syndrome. *Mol Ther Methods Clin Dev*. 2021;23:158–168.
22. Segel M, Lash B, Song J, *et al*. Mammalian retrovirus-like protein PEG10 packages its own mRNA and can be pseudotyped for mRNA delivery. *Science*. 2021;373:882–889.